Persistent benzofuran radical cations in solution. A cyclic voltammetry and EPR/ENDOR study

Michael Schmittel,*[,a] Georg Gescheidt,*[,b] Lennart Eberson[c] and Holger Trenkle[a]

[a] *Institut für Organische Chemie, Universität Würzburg, Am Hubland, D-97074 Würzburg, Germany*
[b] *Institut für Physikalische Chemie, Universität Basel, Klingelbergstr. 80, CH-4056 Basel, Switzerland*
[c] *Chemical Center, Lund University, PO Box 124, S-221 00 Lund, Sweden*

The persistent benzofuran radical cations B1$^{\bullet+}$–B4$^{\bullet+}$ have been generated by electrochemical or chemical oxidation. The lifetimes of the radical cations have been determined by UV spectroscopy and cyclic voltammetry investigations, and their structures established by EPR and ENDOR spectroscopy.

Introduction

Benzofurans **B** can be readily obtained in good yields from the sterically congested β,β-dimesityl enol derivatives **E** [X = H, COR′, SiR′$_3$, TiCp$_2$Cl, and PO(OR′)$_2$] under oxidative conditions, a reaction that is initiated by mesolytic bond cleavage of the corresponding radical cations.[1] For example, deprotonation[2] of the enol radical cation **E**$^{\bullet+}$ (X = H) or O–Si bond cleavage of **E**$^{\bullet+}$ (X = SiR′$_3$) leads to an α-carbonyl radical, which cyclises after one-electron oxidation to the cation **C**$^+$. We have established that the cyclisation proceeds on a fast time scale ($k > 2.5 \times 10^4$ s^{-1} for system **2**),[3] and that the subsequent 1,2-methyl-shift is rate-determining (*ca.* 0.1 s^{-1} at 25 °C).[1b]

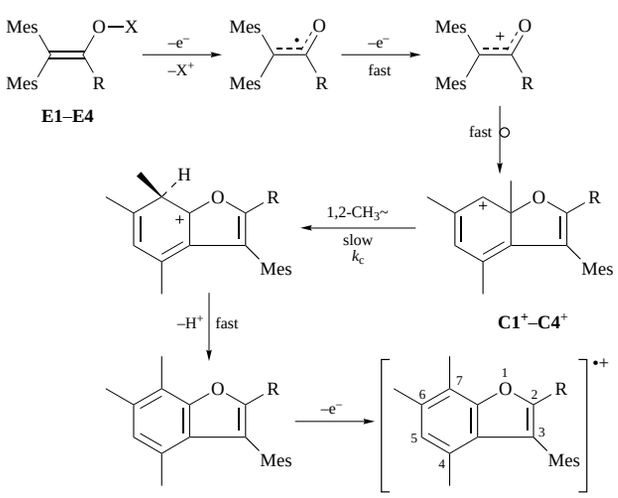

Scheme 1 Mechanism of benzofuran formation from enol derivatives **E** [X = H, COR′, SiR′$_3$, TiCp$_2$Cl and PO(OR′)$_2$]

In this context, we learned a while ago that benzofuran radical cations **B**$^{\bullet+}$ are persistent on the time scale of the cyclic voltammetry (CV) experiment, but we have never sought to characterise these radical cations in more detail. Herein, we now want to present a detailed investigation on the kinetic stability and on the electronic structure of **B1**–**B4**$^{\bullet+}$ using EPR/ENDOR, CV and UV techniques. Interestingly, this seems to constitute the first characterisation of benzofuran radical cations in solution, since only some related dibenzofuran radical cations have been described so far.[4]

Results

Benzofuran formation from enol derivatives

Oxidation of enol carbamate **E3** [1f] [R = Ph, X = C(O)NHBu^t] with 2,3-dichloro-5,6-dicyanoquinone (DDQ) in dichloromethane–trifluoroacetic acid (TFA)[5] at −20 °C led to a red solution without EPR activity. However, when the experiment was repeated using an excess of DDQ, the originally red solution slowly turned blue and an EPR signal could be observed. At −20 °C, the conversion of the red solution, which exhibited UV absorption bands at 360, 428 and 509 nm, into the blue solution was monitored by simultaneous UV–VIS and EPR spectroscopy.[6] Within 50 min the absorption bands at 360 and 509 nm decreased, while two new absorption bands at 628 and 688 nm increased (Fig. 1). An isosbestic point at $\lambda = 585$ nm is indicative of a clean reaction. From the decrease of the 509 nm absorption, the overall time constant of the conversion was determined to $k_c = 1.8 \times 10^{-4}$ s^{-1} (−20 °C). In the same manner as the new absorption bands emerged, an increase in the intensity of the EPR signal was observed, revealing that the 628 and 688 nm bands stem from a novel odd-electron species. As the same EPR signal could be recorded immediately after oxidation of the parent **B3**, the absorptions at 628 and 688 nm should be due to **B3**$^{\bullet+}$. Based on our former investigations[7] on persistent cations **C**$^+$ (R = C$_6$H$_4$NMe$_2$) the absorptions at 360, 428 and 509 nm can be rather confidently assigned to the cyclohexadienyl cation **C3**$^+$. Hence, the rate constant $k_c = 1.8 \times 10^{-4}$ s^{-1} at −20 °C can be attributed to the 1,2-methyl shift of **C3**$^+$ in the enol oxidation reaction (Scheme 1), because the subsequent deprotonation and oxidation of **B3** should be much more rapid under our conditions.

Lifetime of the benzofuran radical cations

The benzofurans exhibit partially reversible waves in the cyclic voltammograms in acetonitrile at room temperature, enabling the determination of the half-wave potentials (Table 1).[8] A closer inspection revealed that the i_{pc}/i_{pa} ratio increases with faster scan rates, approaching asymptotically the value 1 for a completely reversible one-electron transfer.

The rate constants assigned to the follow-up reaction, k_f, of **B1**$^{\bullet+}$ and **B2**$^{\bullet+}$ determined with the help of the Nicholson–Shain formalism[9] are 6.1×10^{-2} s^{-1} (**B1**$^{\bullet+}$, CH$_3$CN–Bu$_4$NPF$_6$), 1.2×10^{-2} s^{-1} (**B1**$^{\bullet+}$, CH$_2$Cl$_2$–Bu$_4$NPF$_6$) and 3.0×10^{-3} s^{-1}

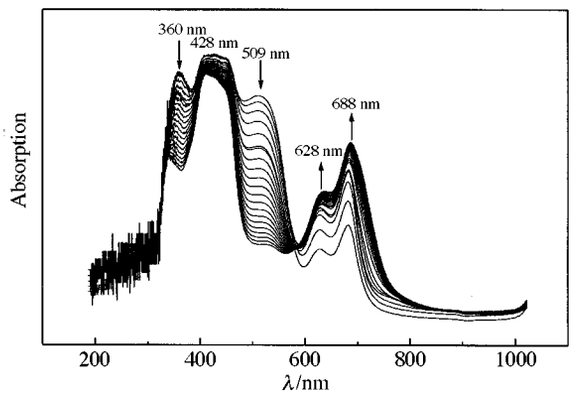

Fig. 1 UV–VIS-detection of the formation of $\mathbf{B3}^{\bullet+}$. The spectra were recorded at −20 °C at intervals of 2 min.

($\mathbf{B2}^{\bullet+}$, CH_3CN–Bu_4NPF_6, 0 °C). Addition of up to 10 equivalents of methanol had no significant effect on the reversibility of the waves. In contrast, addition of two equivalents of the sterically hindered base 2,6-di-*tert*-butylpyridine caused a decrease of the I_{pc}/I_{pa} ratio, indicating that under such conditions the follow-up reaction is accelerated. The aryl-substituted benzofurans **B3** and **B4** showed reversible redox waves independent of the scan rate, thus the radical cations $\mathbf{B3}^{\bullet+}$ and $\mathbf{B4}^{\bullet+}$ should have considerably longer life-times than $\mathbf{B1}^{\bullet+}$ and $\mathbf{B2}^{\bullet+}$. As a consequence, the kinetics of their follow-up reactions were not measured, but an upper limit of $k_f < 10^{-3}$ s^{-1} in acetonitrile at room temperature can be predicted.

After one-electron oxidation of **B2** with tris-2,4-dibromophenylaminium hexachloroantimonate[10] (TDBPA, $E_{1/2} = 1.14$ V_{Fc}), a dark blue solution was obtained ($\lambda_{max} = 590$, 628 nm), assigned to $\mathbf{B2}^{\bullet+}$, that decayed over a period of *ca.* 1 h. In contrast, when 4-tolylthallium(III)bis(trifluoroacetate) was used as oxidant for **B2** in 1,1,1,3,3,3-hexafluoropropan-2-ol (HFP), a deep blue solution of $\mathbf{B2}^{\bullet+}$ resulted, which proved persistent for several days at room temperature as judged by EPR. This observation confirms the excellent radical cation stabilising properties of HFP.[11]

Preparative one-electron oxidation of **B1** with thianthrenium perchlorate (TPC, $E_{1/2} = 0.95$ V_{Fc}) or preparative scale electrolysis in the presence of methanol provided the methoxy-substituted product **5**, while in the case of **B2**, only the unreacted substrate could be isolated.

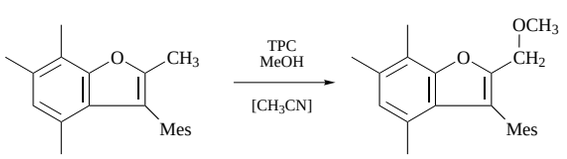

B1 **5**

Scheme 2 One-electron oxidation of **B1**

EPR and ENDOR spectra

The EPR spectra of the benzofuran radical cations were obtained after oxidation of the corresponding enols[2] or enol carbamates[1f] in dichloromethane–TFA acid or HFP with an excess of DDQ or thallium(III)trifluoroacetate. Direct oxidation of the benzofurans (**B1**–**B4**), synthesised by one-electron oxidation of the corresponding enols, yielded identical EPR spectra. In addition, ENDOR and general-TRIPLE spectra could be recorded allowing the direct determination of the ^1H hyperfine coupling constants, a_H, and their relative signs (Table 2). The experimental EPR spectra could readily be simulated using the ENDOR data (Figs. 3–6).

Discussion

Stability of the benzofuran radical cations

The kinetic stability of the benzofuran radical cations increases when the 2-methyl substituent (**B1**) is replaced by 2-*tert*-butyl (**B2**) or aryl groups (**B3, B4**). Since the kinetic measurements show that deprotonation is the primary reaction pathway of both the methyl (**B1**) and the *tert*-butyl-substituted (**B2**) benzofuran radical cation, it seems reasonable to conclude that the 2-methyl group is the most acidic position in $\mathbf{B1}^{\bullet+}$. This proposal is indeed corroborated by finding product **5** after one-electron oxidation of **B1**. After deprotonation of $\mathbf{B1}^{\bullet+}$, the resulting radical is oxidised to the corresponding cation, which is trapped by methanol as nucleophile. The fact that methanol concentration has no effect on the lifetime of the radical cations can be easily explained by this mechanism, as deprotonation is the rate-determining step in the reaction sequence, in agreement with the CV results in the presence of di-*tert*-butylpyridine.

Table 1 Half-wave potentials of benzofurans and UV data for their radical cations[a]

	B1	B2	B3	B4
E_2^1/V *vs.* Fc[8]	0.91	0.93	0.84	0.94
λ_{max}/nm (radical cation)	369, 576	344, 590, 628	313, 427, 628, 688	329, 482, 743

[a] Generated by oxidation with $Tl(CF_3COO)_3$ in TFA.

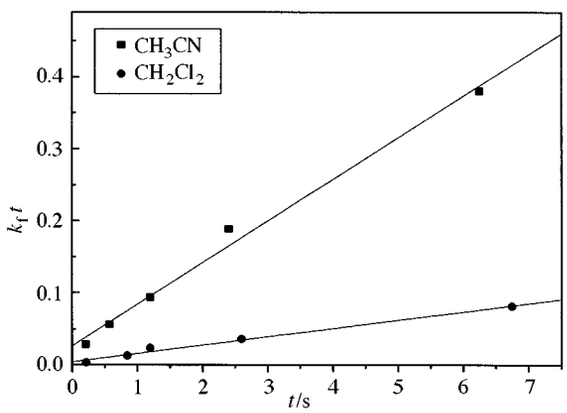

Fig. 2 $k_f t$ *vs.* t plot for the determination of the follow-up rate constant of $\mathbf{B1}^{\bullet+}$ at ambient temperature

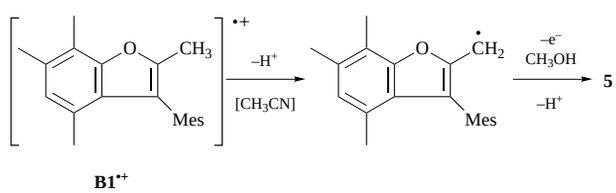

$\mathbf{B1}^{\bullet+}$

Scheme 3 Formation of **5**

The benzofuran radical cations $\mathbf{B2}^{\bullet+}$, $\mathbf{B3}^{\bullet+}$ and $\mathbf{B4}^{\bullet+}$ are thus expected to deprotonate in the less acidic 4-, 6- or 7-methyl positions, coinciding with an increase in their stability. Not surprisingly, one-electron oxidation failed to yield SET products because these follow-up deprotonations are not sufficiently rapid.

EPR and ENDOR spectra

To obtain an insight into the electron distribution of the radical cations $\mathbf{B1}^{\bullet+}$–$\mathbf{B4}^{\bullet+}$ their geometry was calculated with AM1[12] and the isotropic hyperfine coupling constants, a_H, were determined by single-point density functional theory (DFT)[13,14] calculations using Becke's three-parameter hybrid method with Hartree–Fock using the Lee, Yang and Parr correlation functional (B3LYP)[15] with a 6-31G* basis set (GAUSSIAN 94).[16] The experimental and the calculated values are shown in Table 2. In most cases, a straightforward assignment of a_H is possible based on the computed values.

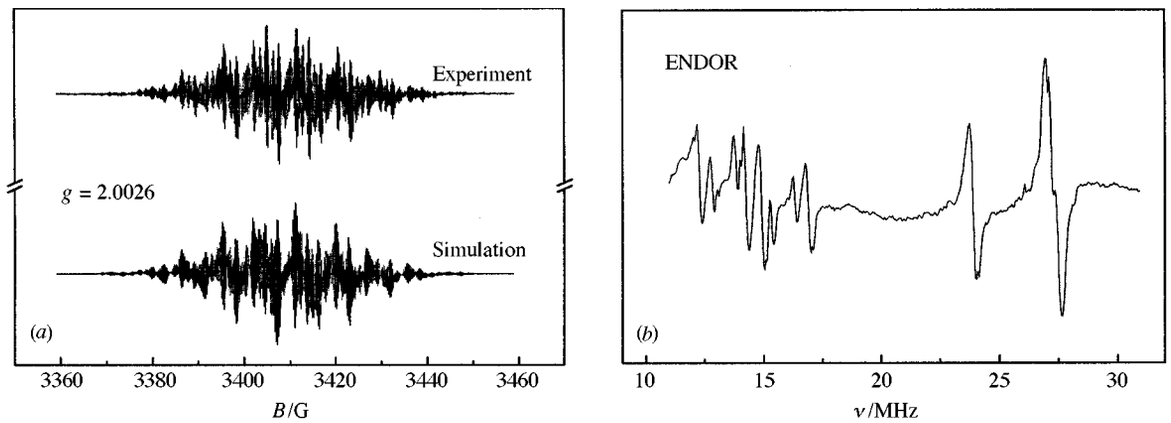

Fig. 3 EPR (*a*: top, experiment; bottom, simulation) and (*b*) ENDOR spectra of benzofuran radical cation **B1**$^{\bullet+}$ [solvent, HFP; oxidant $Tl(OOCCF_3)_3$; $T = 283$ K]

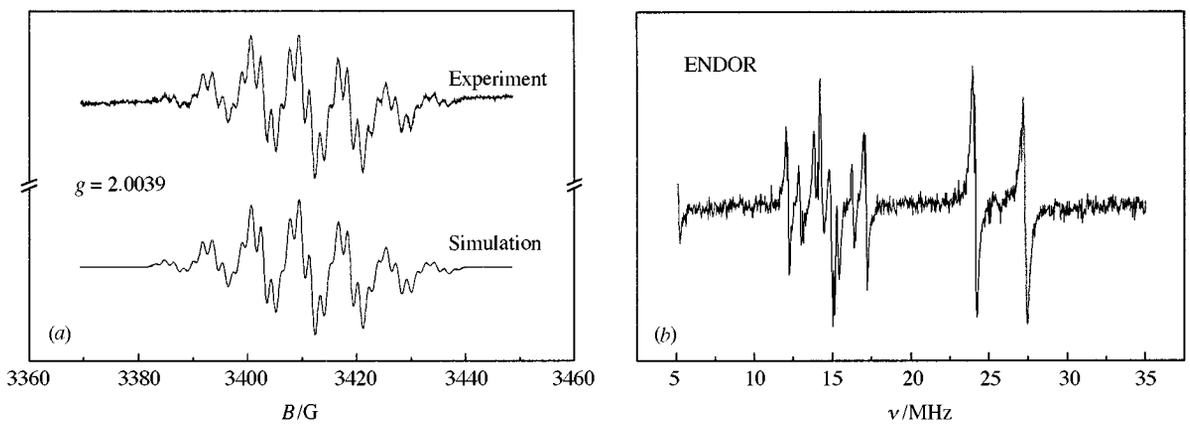

Fig. 4 EPR (*a*: top, experiment; bottom, simulation) and (*b*) ENDOR spectra of benzofuran radical cation **B2**$^{\bullet+}$ [solvent, CH_2Cl_2; oxidant $Tl(OOCCF_3)_3$; $T = 253$ K]

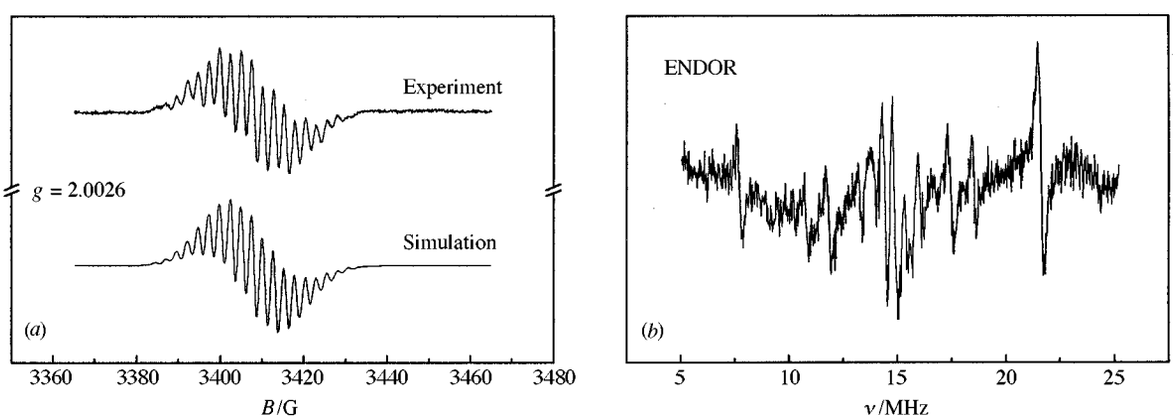

Fig. 5 EPR (*a*: top, experiment; bottom, simulation) and (*b*) ENDOR spectra of benzofuran radical cation **B3**$^{\bullet+}$ [solvent, CH_2Cl_2; oxidant $Tl(OOCCF_3)_3$; $T = 253$ K]

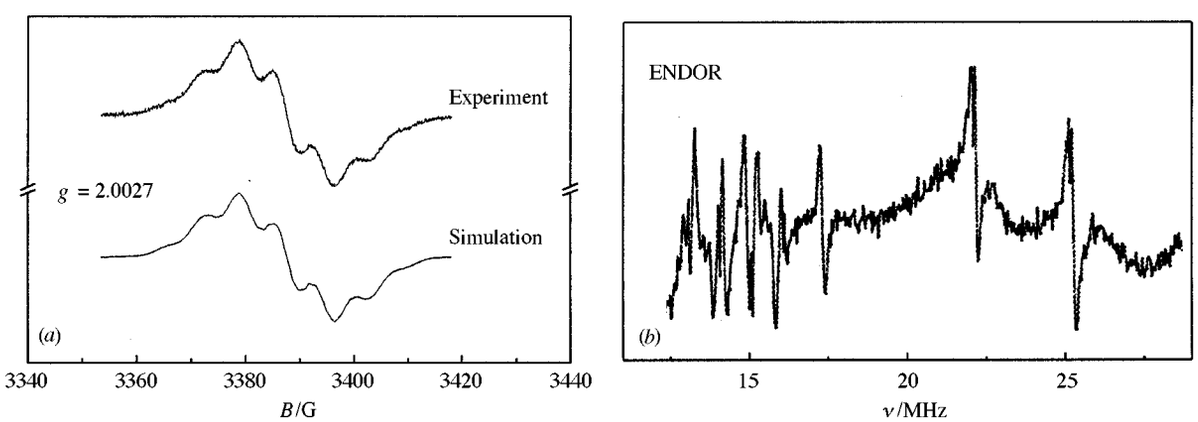

Fig. 6 EPR (*a*: top, experiment; bottom, simulation) and (*b*) ENDOR spectra of benzofuran radical cation **B4**$^{\bullet+}$ [solvent, HFP; oxidant $Tl(OOCCF_3)_3$; $T = 283$ K]

Table 2 Hyperfine data for radical cations **B1**–**B4** from EPR, ENDOR and general TRIPLE spectra and calculated a_H values (AM1//B3LYP-6.31G*)

	Position	a_H (experimental)/G	a_H (calculated)/G	
B1$^{\bullet+}$	CH_3–C(2)	+8.96	+11.3	
g = 2.0026	CH_3–C(6)	+8.94	+8.8	
	CH_3–C(4)	+6.65	+7.7	
	CH_3–C(7)	+1.66	+1.9	
	H–C(5)	+1.25	+2.0	
	$2CH_3$ *ortho* (mesityl)–C(3)	+0.52	+0.2	
	CH_3 *para* (mesityl)	+0.25	+0.1	
	2 H *meta* (mesityl)–C(3)	+0.05	+0.8	
B2$^{\bullet+}$	$(CH_3)_3C$–C(2)	+0.08	+0.2	
g = 2.0039	CH_3–C(6)	+9.10	+8.7	
	CH_3–C(4)	+6.80	+7.8	
	CH_3–C(7)	+1.79	+1.8	
	H–C(5)	+1.21	+2.1	
	CH_3 *para* (mesityl)–C(3)	+0.52	+0.1	
	$2CH_3$ *ortho* (mesityl)–C(3)	+0.18	+0.2	
	2 H *meta* (mesityl)–C(3)	+0.05	+0.9	
			conformation *A*	conformation *B*
B3$^{\bullet+}$	3 H *ortho*/*para* phenyl–C(2)	−0.49	−2.8/−3.8	−0.2/−0.1
g = 2.0026	2 H *meta* phenyl–C(2)	+0.15	+1.2	+0.8
	CH_3–C(6)	+4.99	+7.6	+6.1
	CH_3–C(4)	+4.99	+5.9	+6.5
	CH_3–C(7)	+2.01	+0.1	+1.5
	H–C(5)	+1.03	+1.9	+1.7
	CH_3 *para* (mesityl)–C(3)	+2.79	0.0	+2.9
	2 CH_3 *ortho* (mesityl)–C(3)	+2.79	+0.1	+1.4
B4$^{\bullet+}$	CH_3 *para* (mesityl)–C(2)	+0.81	+1.7	
g = 2.0027	2 CH_3 *ortho* (mesityl)–C(2)	+0.57	+0.4	
	CH_3–C(6)	+7.58	+5.9	
	CH_3–C(4)	+5.41	+4.9	
	CH_3–C(7)	+0.90	+1.1	
	H–C(5)	+1.97	+0.7	
	CH_3 *para* (mesityl)–C(3)	+0.22	+3.9	

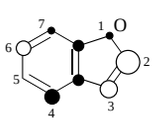

Fig. 7 Shape of the HOMO of an unsubstituted benzofuran according to Hückel MO calculations [heteroatom parameters h(O) = 2.0, k (CO) = 1.0, the O atom contributing two electrons to the π system]

The spin distribution in **B1**$^{\bullet+}$–**B4**$^{\bullet+}$ calculated by the AM1/DFT procedure is roughly reproduced by the shape of the highest occupied molecular orbital (HOMO) of an unsubstituted benzofuran calculated by the Hückel (HMO) method (Fig. 7). To facilitate the discussion we will refer to this highly simplified picture.

From the shape of the HOMO it can be anticipated that the highest spin population is found at C(2) followed by C(3), C(6) and C(4). The methyl group at C(7) is predicted to possess a small coupling constant and π–π polarisation should lead to a positive sign for a_H assigned to the H atom at C(5). With mesityl being the substituent at C(3), the relative orientation of the benzofuran and the mesityl π systems will control the amount of delocalisation. The conformations of the aryl substituents will also be decisive for the extent of spin population which can be transferred to the phenyl or mesityl group at C(2) in **B3**$^{\bullet+}$ and **B4**$^{\bullet+}$.

For the benzofuran radical cation **B1**$^{\bullet+}$ it is straightforward to assign the highest coupling constant of 8.96 G to the three equivalent protons of the methyl group at C(2). The mesityl substituent at C(3) is twisted out of the plane of the benzofuran π system; consequently, although the size of the coefficient at C(3) is considerable, the DFT predictions for the a_H of the *ortho* and *para* methyl groups indicate only small values (Table 2). Thus, the a_H value of 8.94 G is assigned to the methyl group at C(6) followed by 6.65 G for the methyl group at C(4). The a_H value of 1.25 G assigned to the proton at C(5) is in good agreement with the DFT calculated value. According to the calculations, the sign of all these a_H values should be positive; this is corroborated by a general-TRIPLE experiment establishing an identical sign for all a_H values.[17] In the case of **B2**$^{\bullet+}$ one of the large three-proton a_H values is missing and the a_H value of 9.10 and 6.80 G allotted to three equivalent protons of the methyl groups at C(6) and C(4) remain almost unaltered if compared with **B1**$^{\bullet+}$. The additional a_H value detected by the ENDOR technique are assigned based on the DFT calculations (Table 2).

When the substituents at C(2) are aromatic as in **B3** (phenyl) and **B4** (mesityl), electron delocalisation over a greater number of centres becomes possible. Whereas the singly occupied orbital retains its shape in the parent benzofuran moiety, a considerable amount of spin can be found in the aryl substituents of **B3**$^{\bullet+}$ and **B4**$^{\bullet+}$. For **B3**$^{\bullet+}$, AM1 calculations indicate that the energy hypersurface is very shallow when different orientations of the phenyl and the mesityl substituent are taken into account. Therefore we have calculated the Fermi contact terms of **B3**$^{\bullet+}$ based on two geometries. In the first conformation the phenyl group is almost coplanar with the benzofuran π system whereas the mesityl moiety is oriented perpendicular to the remaining π system (conformation *A*). This orientation is reversed in the second conformation: here the mesityl and the benzofuran π systems are coplanar and the phenyl group is twisted outside the benzofuran π plane (conformation *B*). In Table 2 the a_H values calculated by the B3LYP functional based on conformations *A* and *B* are compared to the experimental values. It is evident that the a_H values based on conformation *B* are in better agreement with the experiment than those of conformation *A*. Delocalisation of spin into the mesityl substituent causes a decrease in the coupling constants of the protons in the methyl group at C(6) from *ca*. 9 G in **B1**$^{\bullet+}$ and **B2**$^{\bullet+}$ to *ca*. 5 G in **B3**$^{\bullet+}$ with the remaining a_H values following the same trend. None of the two mesityl groups in **B4**$^{\bullet+}$ can adopt a coplanar

Table 3 Kinetic CV data for $\mathbf{B1}^{\bullet+}$

$\mathbf{B1}^{\bullet+}$ in CH_3CN					$\mathbf{B1}^{\bullet+}$ in CH_2Cl_2				
v/mV s^{-1}	l_{pc}/l_{pa}	$k_f t$	t/s	$l_{pa}/v^{\frac{1}{2}}$	v/mV s^{-1}	l_{pc}/l_{pa}	$k_f t$	t/s	$l_{pa}/v^{\frac{1}{2}}$
20	0.712	0.380	6.25	1.04	20	0.921	0.081	6.75	1.10
50	0.832	0.188	2.40	0.95	50	0.968	0.036	2.60	1.05
100	0.908	0.093	1.20	0.90	100	0.987	0.023	1.20	1.02
200	0.947	0.056	0.58	0.88	200	0.993	0.013	0.85	0.99
500	0.968	0.028	0.21	0.87	500	0.995	0.003	0.22	0.96

arrangement with the benzofuran π system; therefore, the delocalisation of spin into these two moieties is hindered. This is clearly borne out by the increased values of a_H assigned to the methyl protons at C(6) and C(4). Still, these values do not reach the a_H value established for the derivatives $\mathbf{B1}^{\bullet+}$ and $\mathbf{B2}^{\bullet+}$ with aliphatic substituents at C(2).

Due to the higher conformational flexibility of **B3** and **B4** it is not surprising that the calculated a_H values indicate a less pronounced agreement with their experimental counterparts as for **B1** and **B2** where the minimum geometries are much better defined. Still, the combination of the AM1 (geometry) and DFT 3BLYP (Fermi contact) procedures renders possible a satisfactory identification of the rather large and non symmetric radical cations $\mathbf{B1}^{\bullet+}$–$\mathbf{B4}^{\bullet+}$.

Conclusions

The structures of the radical cations $\mathbf{B1}^{\bullet+}$–$\mathbf{B4}^{\bullet+}$ established by EPR spectroscopy are in very good agreement with the assumptions stated for their stability. The persistent benzofurans $\mathbf{B3}^{\bullet+}$ and $\mathbf{B4}^{\bullet+}$ possess a reduced amount of spin population in the benzofuran π system due to delocalisation into the aromatic substituents. This reduces the tendency of the benzofuran radical cations to undergo deprotonation reactions or nucleophilic attack.[18]

Experimental

Materials

The enol derivatives and benzofurans were synthesised following procedures described in the literature.[1,2] Dichloromethane for CV and EPR was distilled from P_2O_5 and filtered over basic alumina. Acetonitrile for CV was distilled from CaH_2. All other chemicals were of commercial quality.

Cyclic voltammetry

In a glove box tetra(*n*-butyl)ammonium hexafluorophosphate (232 mg, 600 μmol) and the electroactive species (6 μmol) were placed into a thoroughly dried CV cell. At a high purity argon line acetonitrile or dichloromethane (6.0 cm^3) was added through a gas-tight syringe. A 1 mm platinum disc working electrode, a Pt wire counter electrode and a Ag pseudo reference electrode were then placed into the solution. The cyclic voltammograms were recorded at various scan rates using different starting and switching potentials. For a determination of the oxidation potentials, ferrocene was added as the internal standard ($E_{1/2} = 0.39$ V *vs*. SCE). Cyclic voltammograms were recorded using a Princeton Applied Research Model 362 potentiostat with an Philips model PM 8271 XYt-recorder. The l_{pc}/l_{pa} values were determined by the equation of Nicholson.[19]

EPR/ENDOR spectra

Samples were prepared in sealed Pyrex glass tubes using high vacuum techniques. EPR and ENDOR spectra were recorded on a Bruker ESP300 spectrometer. Simultaneous UV–VIS spectra were measured on a J&M Tidas fibre-optic diode array spectrometer. EPR simulations were performed using the WinSim simulation program by D. Duling (freeware from the National Institute of Health) .

UV–VIS spectra

UV–VIS spectra were recorded on a Perkin-Elmer Lambda 19 UV–VIS–NIR spectrometer in trifluoroacetic acid using thallium(III)trifluoroacetate as oxidant. Extinction coefficients have not been determined.

One-electron oxidation of B2

According to a previously described method,[2] **B2** was oxidised with 200 mol% of thianthrenium perchlorate to yield **5**. δ_H($CDCl_3$, 250 MHz) 1.84 (s, 3 H, *p*-mes-CH_3), 2.00 (s, 6 H, *o*-mes-CH_3), 2.32 (2 s, 6 H, 4-CH_3, 6-CH_3), 2.42 (s, 3 H, 7-CH_3), 3.33 (s, 3 H, OCH_3), 4.24 (s, 2 H, CH_2O), 6.72 (s, 1 H, 5-H), 6.90 (s, 2 H, mes-H); *m*/*z* for M^+ 322 (60%).

Acknowledgements

We gratefully acknowledge the financial support by the Deutschen Forschungsgemeinschaft (SFB 347). In addition, we are most indebted to the Fonds der Chemischen Industrie for the continuous support for our research. We thank Dipl. Chem. Rolf Söllner (University of Würzburg) for the preparation of **B1**, Rohit Batra and Frederique Barbosa (University of Basel) for performing the quantum mechanical calculations.

References

1 (*a*) M. Schmittel, G. Gescheidt and M. Röck, *Angew. Chem*., *Int. Ed. Engl*., 1994, **33**, 1961; (*b*) M. Schmittel, J. Heinze and H. Trenkle, *J. Org. Chem.*, 1995, **60**, 2726; (*c*) M. Schmittel, M. Keller and A. Burghart, *J. Chem. Soc.*, *Perkin Trans. 2*, 1995, 2327; (*d*) M. Schmittel and R. Söllner, *Angew. Chem.*, *Int. Ed. Engl*., 1996, **35**, 2107; (*e*) M. Schmittel, J.-P. Steffen and A. Burghart, *Chem. Commun.*, 1996, 2349; (*f*) M. Schmittel and H. Trenkle, *Chem. Lett.*, 1997, 299.
2 (*a*) M. Schmittel and M. Röck, *Chem. Ber.*, 1992, **125**, 1611; (*b*) M. Röck and M. Schmittel, *J. Prakt. Chem.*, 1994, **336**, 325.
3 M. Röck and M. Schmittel, *J. Chem. Soc.*, *Chem. Commun.*, 1993, 1739.
4 L. Eberson, M. P. Hartshorn, O. Persson, F. Radner and C. J. Rhodes, *J. Chem. Soc.*, *Perkin Trans. 2*, 1996, 1289.
5 A. G. Davies and K.-M. Ng, *Aust. J. Chem.*, 1995, **48**, 167.
6 G. Gescheidt, *Rev. Sci. Instr.*, 1994, **65**, 2145.
7 M. Schmittel and A. Langels, *Angew. Chem.*, *Int. Ed. Engl*., 1997, **36**, 392.
8 All oxidation potentials are reported *versus* the ferrocene/ferrocenium couple. To obtain values against SCE, simply add +0.39 V.
9 R. S. Nicholson and I. Shain, *Anal. Chem.*, 1964, **36**, 706.
10 E. Steckhan, *Top. Curr. Chem.*, 1987, **142**, 1.
11 (*a*) L. Eberson, M. P. Hartshorn and O. Persson, *J. Chem. Soc.*, *Perkin Trans. 2*, 1995, 1735; (*b*) L. Eberson, M. P. Hartshorn and O. Persson, *Angew. Chem.*, *Int. Ed. Engl.*, 1995, **34**, 2268; (*c*) L. Eberson, M. P. Hartshorn and O. Persson, *J. Chem. Soc.*, *Perkin Trans. 2*, 1996, 141.
12 M. J. S. Dewar, E. G. Zoebisch, E. F. Healy and J. J. P. Stewart, *J. Am. Chem. Soc*., 1985, **107**, 3902.
13 W. Kohn, A. D. Becke and R. G. Parr, *J. Phys. Chem.*, 1996, **100**, 12 974 and references. cit. therein.
14 R. Batra, B. Giese, M. Spichty, G. Gescheidt and K. N. Houk, *J. Phys. Chem.*, 1996, **100**, 18 371.
15 A. D. Becke, *J. Chem. Phys.*, 1993, **98**, 5648.
16 M. J. Frisch, G. W. Trucks, H. B. Schlegel, P. M. W. Gill, B. G. Johnson, M. A. Robb, J. R. Cheeseman, T. Keith, G. A. Petersson, J. A. Montgomery, K. Raghavachari, M. A. Al-Laham, V. G. Zakrzewski, J. V. Ortiz, J. B. Foresman, J. Cioslowski, B. B.

Stefanov, A. Nanayakkara, M. Challacombe, C. Y. Peng, P. Y. Ayala, W. Chen, M. W. Wong, J. L. Andres, E. S. Replogle, R. Gomperts, R. L. Martin, D. J. Fox, J. S. Binkley, D. J. Defrees, J. Bake, J. P. Stewart, M. Head-Gordon, C. Gonzalez and J. A. Pople, GAUSSIAN 94, *Revision B.2*; (Pittsburgh PA, 1995); M. J. Frisch, G. W. Trucks, H. B. Schlegel, P. M. W. Gill, B. G. Johnson, M. A. Robb, J. R. Cheeseman, T. Keith, G. A. Petersson, J. A. Montgomery, K. Raghavachari, M. A. Al-Laham, V. G. Zakrzewski, J. V. Ortiz, J. B. Foresman, C. Y. Peng, P. Y. Ayala, W. Chen, M. W. Wong, J. L. Andres, E. S. Replogle, R. Gomperts, R. L. Martin, D. J. Fox, J. S. Binkley, D. J. Defrees, J. Baker, J. P. Stewart, M. Head-Gordon, C. Gonzalez and J. A. Pople, GAUSSIAN 94, *Revision B.3*; (GAUSSIAN, Inc., Pittsburgh PA, 1995).

17 H. Kurreck, B. Kirste and W. Lubitz, *Electron Nuclear Double Resonance Spectroscopy of Radicals in Solution*, VCH, Weinheim, 1988.

18 See also, L. Eberson, R González-Luque, M. Merchán, F. Radner, B. O. Roos and S. Shaik, *J. Chem. Soc.*, *Perkin. Trans. 2*, 1997, 463.

19 R. S. Nicholson, *Anal. Chem.*, 1966, **38**, 1406.

Paper 7/04594H
Received 30*th June* 1997
Accepted 1*st August* 1997